4-16-2021

Defying the Darkness: Countering Cancer with Light

Travis Hankins
Ouachita Baptist University

SENIOR THESIS APPROVAL

This Honors thesis entitled

"Defying the Darkness: Countering Cancer with Light"

written by

Travis Hankins

and submitted in partial fulfillment of
the requirements for completion of
the Carl Goodson Honors Program
meets the criteria for acceptance
and has been approved by the undersigned readers.

_____
Dr. Joseph Bradshaw, thesis director

_____
Dr. Timothy Hayes, second reader

_____
Dr. Amy Sonheim, third reader

_____
Dr. Barbara Pemberton, Honors Program director

April 16, 2021

Defying the Darkness: Countering Cancer with Light

Travis J. Hankins

University Professor: Dr. Joseph E. Bradshaw

Ouachita Baptist University

Table of Contents

Table of Figures

Table of Tables

Glossary

Acid Chloride: An organic compound with the functional group RCOCl, where R represents another group or a hydrogen atom. See (a) illustrated in Figure 1 on page 8.

Alcohol: An organic compound with the functional group ROH, where R represents another group. See (b) illustrated in Figure 1 on page 8.

American Type Culture Collection (ATCC): A nonprofit organization that collects, stores, and distributes standardized reference microorganisms, cell lines, and other materials used in research and development.

Amide: An organic compound with the functional group RCONR'R", where R, R', and R" represent other groups or hydrogen atoms. See (c) illustrated in Figure 1 on page 8.

Amine: An organic compound with the general formula RNR'R", where R, R', and R" represent other groups or hydrogen atoms. See (d) illustrated in Figure 1 on page 8.

Benzene: An organic compound with the molecular formula C_6H_6. See (e) illustrated in Figure 1 on page 8.

Carboxylic Acid: An organic compound with the functional group RCOOH, where R represents another group or hydrogen atom. See (f) illustrated in Figure 1 on page 8.

Electronegativity: A measurement of an atom's tendency to attract a pair of electrons.

Eluent: In chromatography, a solvent used to separate a mixture of compounds; the eluent is chosen based on what the user intends to accomplish with the chromatography.

Ether: An organic compound with the functional group ROR', where R and R' represent other groups. See (g) illustrated in Figure 1 on page 8.

Functional Group: (In Organic Chemistry) substituents comprised of one or more atoms that, when put together in a particular fashion, are responsible for the chemical characteristics of the molecule.

Halogen(ated): An element from group 17 on the periodic table, characterized by their high reactivity; "halogenated" refers to a bond established between a halogen and another atom.

Heterocyclic: Cyclic compound containing at least two different elements in the ring.

LD_{50}: Abbreviation for "Lethal Dose, 50%". In toxicology, this value corresponds to the amount of substance that would need to be administered to kill 50% of the treated population.

Micro- (μ-): The metric system prefix equivalent to a factor of 0.000001 (10^{-6}).

Molar (-M): a unit of concentration equal to one mole (6.022×10^{23} molecules) of a substance in one liter of solution.

Molar Absorptivity Coefficient: An intrinsic physical measurement of how strongly a species absorbs light at a specific wavelength.

Nano- (n-): The metric system prefix equivalent to a factor of 0.000000001 (10^{-9}).

Polar: (Of an atom or molecule) possessing an uneven overall electron distribution that results in an associated unequal distribution of electric charge.

Reflux: A technique used to supply energy to reactions over time without losing large amounts of material to evaporation; the solution is placed in a container and boiled while a condensing column keeps vapor from escaping.

Resonant Frequency: an object's natural, inherent frequency of vibration that is determined by the object's physical parameters; an object can be excited into a vibratory state if placed in the presence of an external influence cycling at its resonant frequency.

Rotary Evaporator (Rotovap): A device used to remove liquids from samples; the device pulls a vacuum, applies heat, and rotates the sample simultaneously which makes evaporation both faster and easier. Rotation of the sample during heating prevents bumping, a phenomenon that occurs when a solution is heated past its boiling point and bubbles spontaneously from within the liquid. This bubbling needs to be prevented if possible, as it can cause potentially violent expulsions.

Sparge (sparging): A synthetic technique that involves pumping an inert gas into a reaction flask to expel other reactive gases which can otherwise produce unfavorable side products.

Spin: An intrinsic type of angular momentum (rotational analog of linear momentum) that certain particles possess. Originally, spin was thought of as the rotation of a particle around some internalized axis; although particles don't actually spin in this fashion, the mental picture is correct as far as the application of the mathematical laws are concerned.

Thin-Layer Chromatography (TLC): A technique used to separate mixtures; unlike column chromatography, TLC does not purify samples but instead is used for identifying components, analyzing purity, and monitoring the progress of reactions.

Triple-Negative Breast Cancer (TNBC): A subtype of breast cancer lacking the estrogen, progesterone, and amplified human epidermal growth factor (HER2) receptors commonly found in breast cancers. This type of cancer is harder to treat than other types of breast cancer due to the lack of these receptors.[8]

Functional Groups

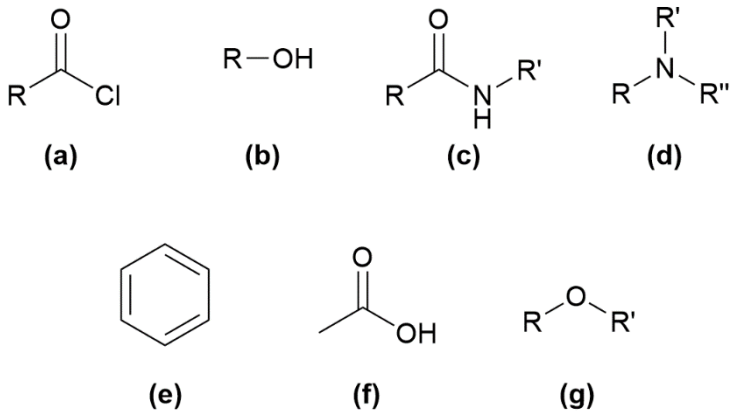

Figure 1: An image of important functional groups discussed in this thesis. Names for each group are listed in the glossary. The placeholder "R" indicates the possibility for further hydrogens or carbon structures, provided that no bonding rules are violated, and redundancies are not formed (ex. one of the "R" groups on an ether (g) cannot be a hydrogen, as this would create an alcohol (b)).

Abstract

Triple-Negative Breast Cancer (TNBC) accounts for upwards of 15% of reported breast cancer cases. This subtype of breast cancer poses a greater threat to those diagnosed as compared to other types of breast cancer due to the lack of treatment options available. Additionally, TNBC grows and spreads faster, tends to be more aggressive, and has a greater chance of recurrence than its counterparts. Altogether, TNBC cases generally have a worse prognosis over other types of breast cancer. Photodynamic therapy (PDT) is currently being researched as a way to treat TNBC. Photodynamic therapy agents are light-activated materials used for localized disease treatment. The compounds known as porphyrins are notable examples of photosensitive agents. Through this project, the novel, water-soluble porphyrin derivative H_2TPP-MorphMeOH was synthesized from the starting materials, H_2TPPC and the amine morpholin-2-yl methanol. Following the synthesis, the compound was purified through liquid chromatography, and then characterized using infrared (IR), nuclear magnetic resonance (NMR), and UV-Vis spectroscopies, and High-Performance Liquid Chromatography (HPLC). Lastly, to determine its utility as a PDT agent, the cytotoxicity of H_2TPP-MorphMeOH was determined using an MTT assay on MDA-MB-231 TNBC cells in the presence and absence of white light.

Background

The research detailed in this thesis investigated the use of porphyrin derivatives as potential photodynamic therapy agents. Specifically, this research focused on the synthesis and analysis of a novel porphyrin with potential phototherapeutic capabilities.

What are Porphyrins?

Porphyrins are a group of organic compounds possessing a characteristically large and planar **heterocyclic** ring as the central component of the molecule. Complex porphyrins can have several substituents attached to the molecular periphery that change the properties of the compound[1]; the basis of this research revolves around this principle.

The term "porphyrin" originated from the Greek word "πορφύρα" (porphyra), meaning purple.[2] Named after their color, porphyrins typically exhibit vibrant hues and, depending on their peripheral substitution, can appear as virtually any color in the visible spectrum (although red and purple occur most frequently, hence the namesake).[3] Interestingly, porphyrins often retain this vibrancy even in very low concentrations, which is an uncommon trait for most compounds; this principle of porphyrins retaining color intensity is utilized in an analytical technique discussed on page 30 and contributes to the efficiency of porphyrins as PDT agents.

The unique structure of porphyrins, specifically the large conjugated (alternating) double bond system and overall modifiability, allows for their impressive utility in chemical and biological systems. Aside from being used for phototherapy, porphyrins are also used as metal binders (ligands), as electron transfer mediums (such as solar cells), and as oxygen transport mediums.[3] The most widely known porphyrin, heme, is an example of

an oxygen transport medium, which exists in hemoglobin.[3] The structure of Porphin, one of the simplest porphyrins, is shown in **Figure 2**; most porphyrins contain a "core" that is structurally similar to this molecule.

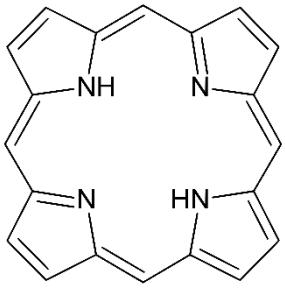

Figure 2: The structure of Porphin, one of the simplest porphyrins.

What is Photodynamic Therapy?

Photodynamic therapy (PDT) is a form of treatment that uses a specific drug called a photosensitizing agent and light to treat various ailments such as esophageal and non-small cell lung cancer.[4] When photosensitizers (PS) are administered and exposed to the appropriate wavelength of light, the drug is excited from its ground state into an excited state, which then produces a type of oxygen known as a singlet oxygen. This singlet oxygen is a reactive oxygen species (ROS) that readily reacts with other molecules in a cell; a buildup of these ROS following the photoactivation of a photodynamic agent damages the DNA, RNA, and proteins within a cell, which induces cell death.[5]

Physicians use tailored photosensitizing agents and specific wavelengths of light to treat different locations throughout the body. The activation wavelengths for photosensitizing agents are unique to the agent, and as the wavelength of light determines the distance into tissue that the light can penetrate (with longer wavelengths of light penetrating further than shorter wavelengths),[6] possessing a diverse array of

photosensitizing compounds with an equally diverse set of activation wavelengths increases the utility of photodynamic therapy.

Studies have concluded that forms of PDT can work as well as surgery or radiation in treating certain types of cancers.[7] Normally, PDT has no long-term side effects, is less invasive, is very precise, doesn't scar tissues, and often costs less than other forms of treatment.[7] However, one of the innate limitations of PDT is that it can only be used in areas of the body where light can reach; this means that it cannot be used on larger cancers or cancers that manifest deep in the body. Additionally, PDT may leave patients sensitive to light for extended periods of time, so precautions must be taken before and after the drugs are administered, such as avoiding direct sunlight and wearing protective clothing when outdoors.[7] However, provided that the tumor is accessible, and the patient is willing to undergo monitoring and limited exposure to sunlight, PDT can be a safe and advantageous alternative to other more invasive or debilitating treatments.[4,7]

Although some PDT agents can be used in treatments for multiple cancers, PS are often designed to combat a particular type; doing so grants specificity towards the treatment and may improve the effectiveness of the PS. In the case of this research project, the PS was designed to be used against **Triple-Negative Breast Cancer**.

Why focus on Triple-Negative Breast Cancer?

Triple-Negative Breast Cancer is a form of cancer lacking the estrogen, progesterone, and amplified HER-2 receptors found in most types of breast cancer.[8] Accounting for 10-20% of reported breast cancer cases, this form of cancer is notably more difficult to treat and eliminate, as the receptors play an essential role in the most common

treatment processes. Cellular receptors are proteins on the nucleus of a cell that receive signals from outside the cell, the signals most often originating from the binding of a key protein or molecule. Normally, once a molecule binds to a receptor, a cellular response is initiated; in the case of the aforementioned receptors, the cellular response is the passage of a signal across the cell membrane.[9] The Centers for Disease Control describe it most succinctly:

> Think of cancer cells as a house. The front door may have three kinds of locks, called receptors – one is for the female hormone estrogen, one is for the female hormone progesterone, and one is for a protein called human epidermal growth factor (HER2). If your cancer has any of these three locks, doctors have a few keys (like hormone therapy or other drugs) they can use to help destroy the cancer cells. But if you have triple-negative breast cancer, it means those locks aren't there.[8]

Lacking these receptors reduces the number of "keys" that can be used during treatment, so research continues to find additional alternatives.

Because modern treatments often use the receptors in cancer cells as pathways for delivery, few medicines have been designed with alternative transport methods in mind. For this reason, a prerequisite characteristic of compounds being synthesized to combat this cancer is high solubility in water without degradation. If the compound used for treatment is water soluble, it can be easily transported through the blood to the target tissue. This characteristic of treatment options, being highly water soluble, is therefore mandatory in the synthesis of an effective form of treatment against TNBC.

Finally, as with all other treatment methods, several criteria must be satisfied by the experimental compound before it can be considered an effective form of treatment

against TNBC (in addition to water solubility). Aside from general safety, concerns of production cost, accessibility, and commercial applicability (how widespread the compound can theoretically be used) also affect the usefulness of any experimental compound. However, concerns of commercial influence and usage become relevant only when an operational compound has been identified.[10] These concerns are therefore beyond the scope of this research project. For the sake of this project, the objective in designing a photodynamic agent is to create a compound cytotoxic enough to kill cancer cells in very low concentrations, but only when exposed to light.

Project Goals

As mentioned earlier, this research focused on the synthesis of a novel water-soluble porphyrin. The overall goal of this project was to synthesize a porphyrin that is water-soluble, possesses strong photosensitizing characteristics, is able to kill cells in very low concentrations once exposed to light, and has little to no cytotoxic effect when left unexposed. This was accomplished by first theorizing a synthetic route for the creation of the porphyrin, then performing the synthesis. Next, the product was isolated from impurities using various purification techniques before moving to characterization via instrumental analysis. Finally, the efficacy of the porphyrin derivative as an anticancer agent was quantified using a cellular metabolic assay. If the compound is found to be a strong anticancer agent, testing will continue in hopes of solidifying its use in photodynamic therapy.

Methods

The production of the final porphyrin occurred through a multistep synthesis that can be grouped into three individual stages. The first step involved the synthesis of 5,10,15,20-tetrakis(4-carboxyphenyl)porphyrin, H_2TPPC, which served as the base molecule for the subsequent reactions. Following this, the porphyrin was transformed through a reaction that produced a **halogenated** intermediate; this intermediate provided ideal chemical properties that facilitated a greater production of the final product. Finally, a reaction on the periphery of the porphyrin core yielded the desired molecule from the halogenated intermediate and the selected **amine**. Following purification by column chromatography, the novel water-soluble photosensitizing agent was ready for analysis and testing.

In comparison to the starting material, the final product, H_2TPP-MorphMeOH, retained the starting internal structure but made significant changes to the molecular periphery. These changes provided the product with the necessary characteristics to function as a PDT agent. The final product is shown in **Figure 3**.

The production of the porphyrin product occurred stepwise over the course of multiple days. A routine synthesis proceeded as detailed in the following sections.

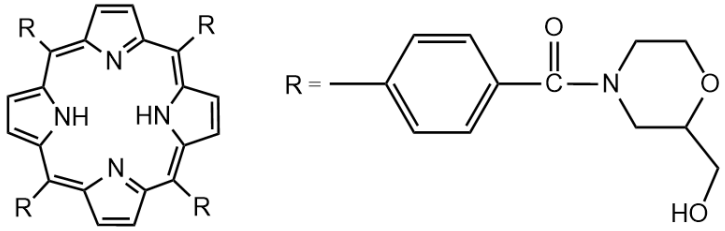

Figure 3: The final product, H_2TPP-MorphMeOH.

Synthesis of H_2TPPC, 5,10,15,20-tetrakis(4-carboxyphenyl)porphyrin

A 3.00 g sample of 4-formylbenzoic acid, a 1.4 mL sample of pyrrole, a ~200 mL volume of propionic acid, and a stir bar were introduced to a 250 mL round-bottom flask. This solution was then stirred and heated under **reflux** conditions for one hour to promote the formation of H_2TPPC. Following reflux, the reaction solution was placed in a freezer overnight. Next, the solution was filtered using a medium Büchner fritted filter and washed with dichloromethane (CH_2Cl_2) before being stored in a vial and dried in a lab oven for one hour. Through this process, crude H_2TPPC was formed. **Figure 4** shows the reaction.

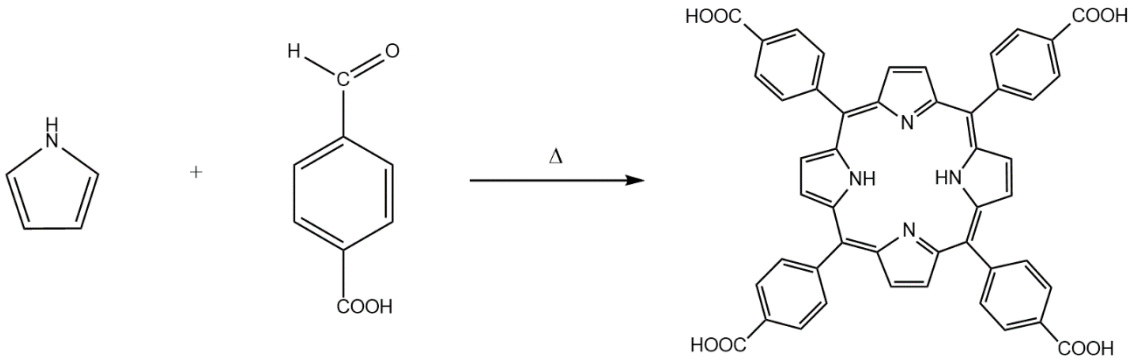

Figure 4: The reaction used to produce the porphyrin, H_2TPPC. From left: pyrrole, 4-formylbenzoic acid, H_2TPPC.

Synthesis of H_2TPP-MorphMeOH

As mentioned earlier, use of a halogenated intermediate facilitates greater yield of the desired **amide** product. The synthesis of the final amide product occurs in two steps; the first reaction employed a standard method for converting carboxylic acids into **acid chlorides** by treatment with thionyl chloride, and the second step reacted the amine with

the acid chloride to form an amide linkage and couple the two reagents. **Figures 5 and 6** show the reactions.

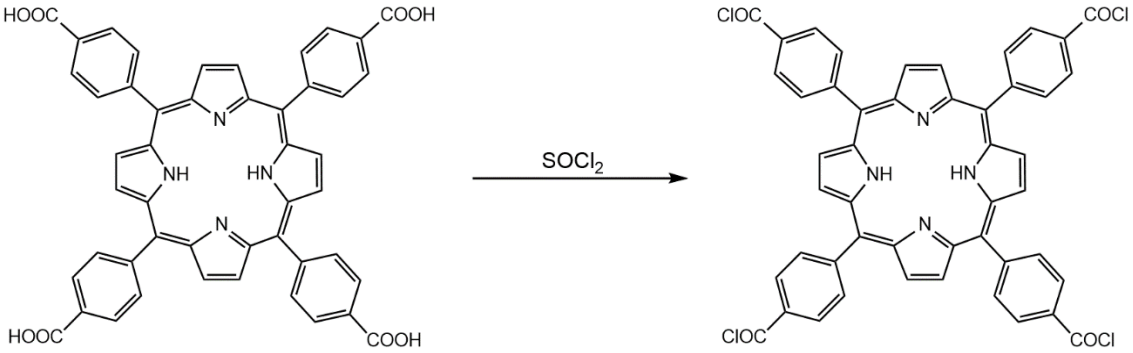

Figure 5: The reaction used to generate the acid-chloride porphyrin intermediate. Performing this reaction changed only the sites in the periphery and did not affect the internal structure.

Glassware was oven dried prior to use. A rubber septum was placed into the round bottom flask opening to prevent atmospheric exposure and the flask was then placed under a nitrogen **sparge**. A 0.25 g sample of H_2TPPC was weighed out and transferred to the flask, followed by ~20 mL of dimethylformamide, DMF, to dissolve the H_2TPPC. With stirring under nitrogen flow, 0.25 mL of thionyl chloride ($SOCl_2$) was introduced to the round bottom flask. This solution was then stirred under nitrogen sparge for one hour. The DMF was subsequently removed under vacuum.

To ensure dryness, methanol was freshly distilled from sodium prior to use. In an oven-dried vial, 0.25 g of morpholin-2-yl methanol was added and dissolved in the dry methanol. Once dissolved, this solution was immediately added to the acid-chloride intermediate under nitrogen sparge. The reaction was stirred for one hour. Subsequently, the methanol was removed under a vacuum by a **rotovap**. Through this process, crude H_2TPP-MorphMeOH was produced. **Figure 6** shows the reaction.

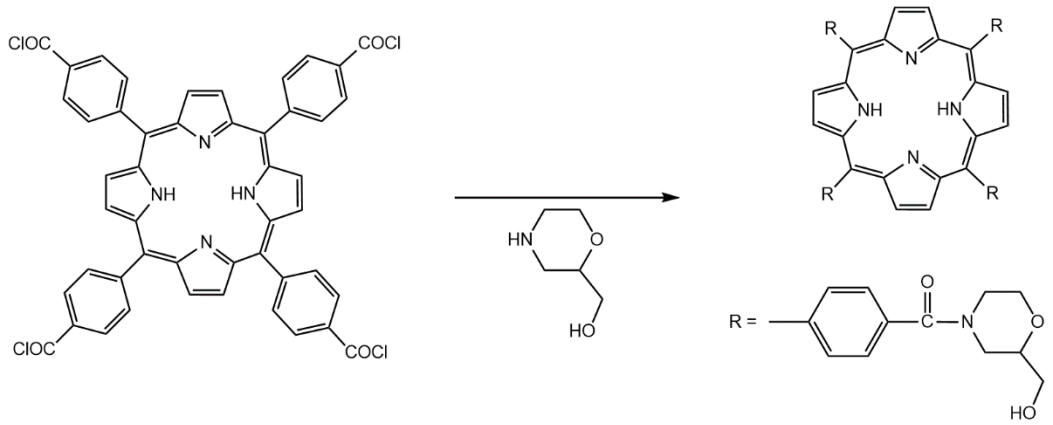

Figure 6: The reaction used to generate the final product, H_2TPP-MorphMeOH. The molecule underneath the reaction arrow is the amine used to perform the reaction, morpholin-2-yl methanol.

Purification by Column Chromatography

Because the reactions used to synthesize the product were not 100% efficient and an excess of amine was used, the final porphyrin product needed to be purified due to traces of unreacted components and byproducts. To isolate the desired compound, the recovered product was subjected to a series of purification steps including syringe filtration and column chromatography. For purification of the product, two different chromatography columns were used; once one column was finished, the purified sample was transferred to the second column and further purified.

The product was first purified using Sephadex LH-20 with methanol and Milli-Q H_2O (50:50) as the eluent. Sephadex LH-20 is a lipophilic or "fat-loving" medium, meaning that molecules dense in the same atoms that comprise fat and oils, particularly carbon and hydrogen, move through the column slower than others. Passing a mixture through it results in a gradual separation of the components based on their interaction with the medium.

After the initial column, the product was further purified using Sephadex G-50 with Milli-Q H_2O as the eluent. Sephadex G-50 separates a mixture of compounds based on their individual size; molecules that are larger move around the Sephadex beads rather than through them, resulting in a gradual separation of the components based on their size.

To quantify the efficiency of the purification step, the refined product was subjected to HPLC analysis, discussed on page 33.

Characterization

To confirm that the compound produced was the desired product, the final compound was subjected to a series of analytical tests to verify the structure of the molecule and quantify the purity of the final product.

Analytical Techniques

Infrared (IR) Spectroscopy

The infrared spectrometer used for characterization was a Thermo Scientific Nicolet iS10 infrared spectrometer with OMNIC 9 analysis software. Infrared spectroscopy was used to verify that the amine was successfully bound to the porphyrin core by identifying signals associated with the amide functional group formed by the reaction shown in **Figure 6**.

In infrared spectroscopy, a sample of a compound is bombarded with infrared radiation with wavelengths spanning 2-25 μm (**micro**meters) and a constant initial intensity; the intensity of each wavelength of light returned from the sample is compared to the initial intensity and then graphed as the percentage transmittance, or the ratio of incoming to outgoing intensity.[11] The principle of this technique stems from the theory that molecules absorb certain wavelengths of light as determined by their molecular structure; based on a number of factors that affect each bond's **resonant frequency**, the presence of particular bonds in the sample will lead to the absorption of certain associated frequencies of infrared light (therefore exciting the molecule into various vibrational states), which will then affect each wavelength's transmittance, and thus yield associated observable changes

in the sample's infrared spectrum. The range of infrared radiation used in this analytical technique is chosen because it possesses the necessary amount of energy to cause the desired bond excitations in the sample.[11] **Figure 7** shows a simplified diagram detailing how infrared spectroscopy works.

To determine if the compound was synthesized as anticipated, the infrared spectrum of both the final product and morpholin-2-yl methanol was taken and compared to verify that they had similar signal patterns.

Because of the structure of morpholin-2-yl methanol (see **Figure 6**), the main signals of concern would be those generated by the alcohol, amine, and ether functional groups. As anticipated based on literature values, the signals for each of these groups, respectively, were identified as the broad signal at 3300 cm^{-1} and the peaks at 1050-1110 cm^{-1}; these will be the reference signal values for the final product IR. The infrared spectrum of morpholin-2-yl methanol is shown in **Figure 8**.

To verify that the amine was bound to the porphyrin core in the final reaction, the IR spectrum of the product was analyzed to see if it contained the associated amide bands.

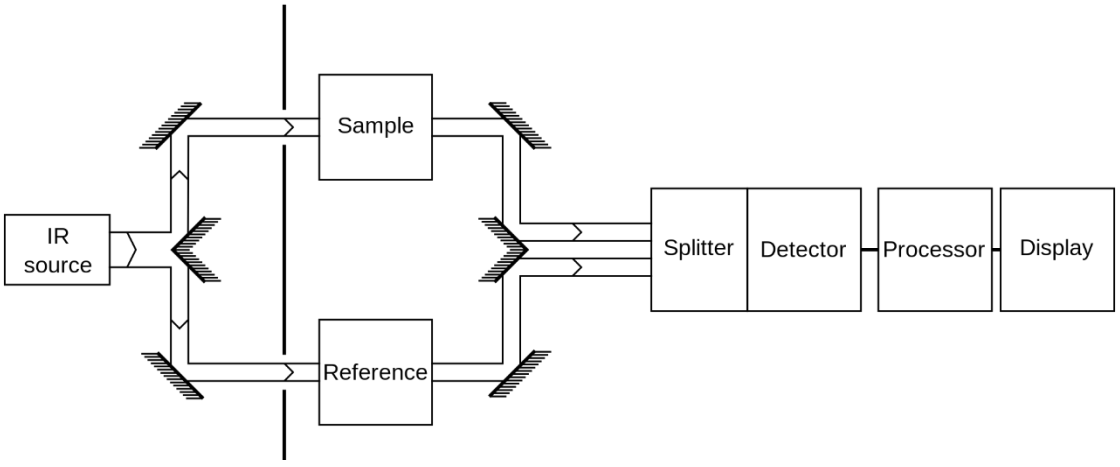

Figure 7: A simplified diagram showing how IR spectroscopy works.[12] This chart depicts a "two-beam" spectrometer, while the instrument used in this research was a "one-beam" – the instrument was pre-calibrated before each analysis which obviated the need for a reference and second beam.

If the two components were properly coupled, the infrared spectrum should contain the predicted regions known as the amide I, amide II, and amide III bands. Unlike the IR spectrum for morpholin-2-yl methanol, there were prominent signals at 1583 cm^{-1}, 1537 cm^{-1}, and 1371 cm^{-1}, which correspond to the amide I, amide II, and amide III bands, respectively[14]; these bands are indicative of a secondary, non-cyclic amide functionality, which is what was anticipated from the proposed synthetic pathway. From this, it was concluded that the amine was properly bound to the porphyrin core in the final reaction. The infrared spectrum of the final product is shown in **Figure 8**.

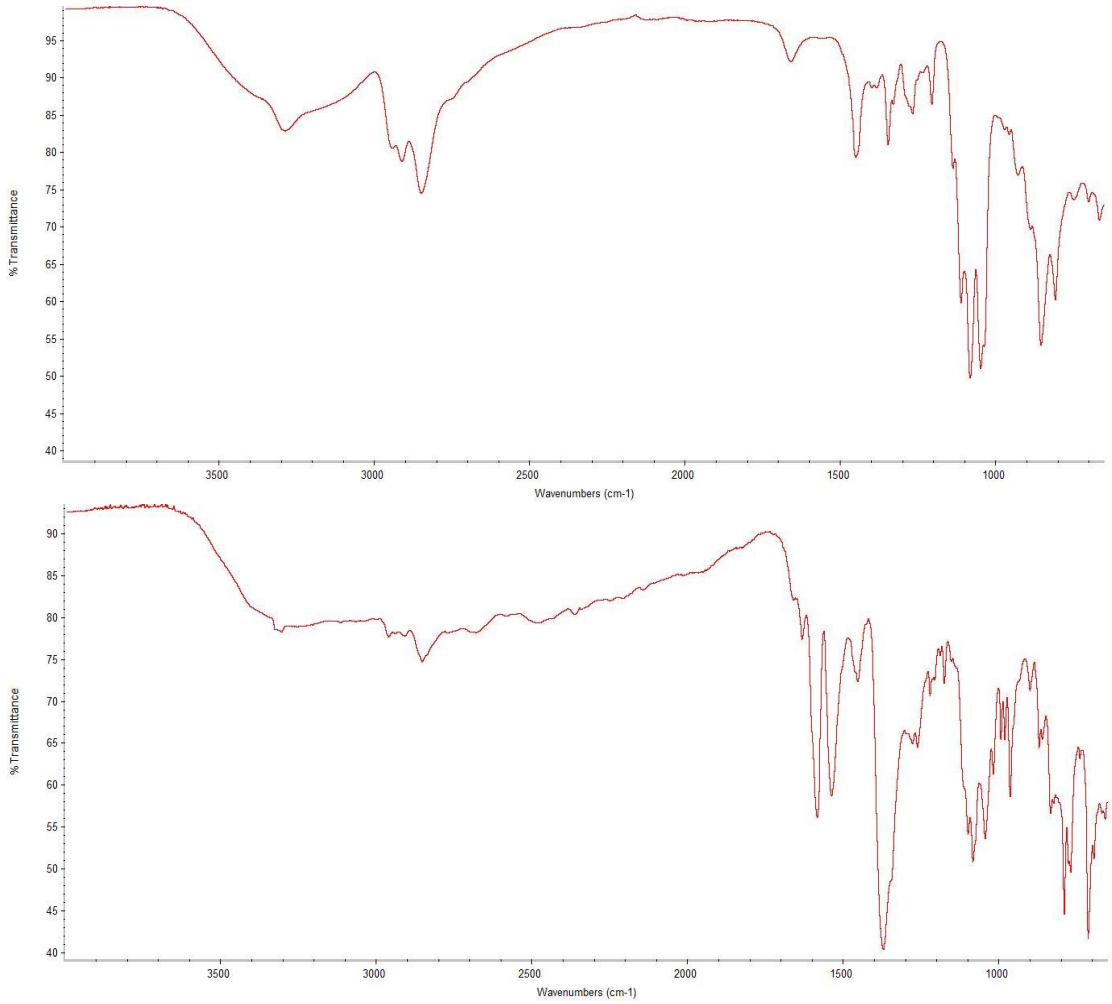

Figure 8: The IR spectra of the amine, morpholin-2-yl methanol (top), and the product, H_2TPP-MorphMeOH (bottom). Although the wavenumbers are aligned, the transmittance scales (y-axis) are not perfectly equal; signals in the amine spectrum are slightly less intense than they appear in comparison to those in the product spectrum.

Nuclear Magnetic Resonance (NMR) Spectroscopy

The nuclear magnetic resonance spectrometer used was an Eft-60 MHz NMR Spectrometer with PNMR analytics software and NMR utility software (NUTS). Supplementary computational NMR spectra were produced using *nmrdb.org*. Again, NMR spectroscopy was used to verify the structure of the final product.

In nuclear magnetic resonance spectroscopy, a sample of a compound is placed within a powerful magnetic field (tens of thousands of times stronger than the Earth's magnetic field); once active, atoms possessing a **spin** align with the external magnetic field. The sample is then irradiated with an electromagnetic pulse comprised of specific radiowave frequencies which causes resonance between the waves and atoms; similar to infrared waves for IR, radiowaves are used because they possess the amount of energy required to cause the desired resonances in the sample. When the waves and atoms interact, the nuclei are deflected from being aligned with the magnetic field; these deflections cause the nuclei to fall perpendicular to the field and rotate, which then induces an electric current in a metal coil surrounding the sample. In effect, the change of the voltage passing through the wire is a direct representation of how the nuclei of the sample are behaving in response to the electromagnetic pulse, which can be monitored and interpreted by the instrument.[15] A number of factors contribute to the frequency of the signals, which cause observable changes in the NMR spectrum; together, all of the various signals from the sample produce a "picture" of the molecule that the NMR spectrum describes. Since many types of nuclei can cause readings, each NMR taken for a sample traditionally focuses on one type of nucleus by isolating the frequencies to use for irradiation. To identify what type of NMR was taken, an indicator is included with the results for quick reference (ex. ^{1}H (hydrogen),

^{13}C (carbon), etc.); the type of analysis used to characterize the product in this research was ^{1}H NMR.[15] **Figure 9** shows a simplified diagram detailing how NMR spectroscopy works.

In the type of analysis used for this research, the signals shown in the NMR spectrum are the result of "deshielded" hydrogens. Hydrogen nuclei attached to or near **electronegative** atoms lose electron density to those atoms and are more susceptible to an external magnetic field's effects; in a sense, nuclei are "shielded" by their electrons, and when the electron density around a nucleus is reduced by a neighboring electronegative atom, the one that loses the density becomes "less shielded", or deshielded. These hydrogen nuclei produce signals that are "downfield" with respect to the reference signal (a signal corresponding to a field offset of 0 ppm produced from a compound called tetramethylsilane (TMS) included in the solvent). Regarding the solvent used to dissolve the compound, because the NMR produced signals based on hydrogens in the solution, a special type of solvent had to be used in place of normal ones. These solvents replace hydrogen with deuterium (^{2}H) in the structure, thus negating the solvent's influence on the

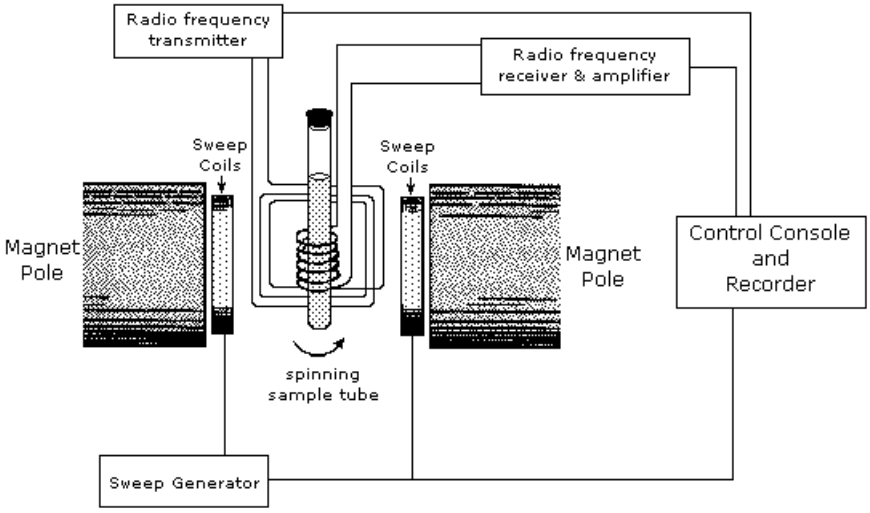

Figure 9: A simplified diagram showing how NMR spectroscopy works.[16] The sample tube is placed in between the poles of the NMR magnet and a recorder measures changes in the magnetic field resultant of nuclear deflections in the sample.

NMR; because they use deuterium in place of hydrogen, the solvents are known as "deuterated" solvents. The solvent used to dissolve the amine was deuterated chloroform ($CDCl_3$) and the solvent used to dissolve the H_2TPP-MorphMeOH was deuterated water (D_2O).

To determine if the final compound was formed, both the ^{1}H NMR spectrum of the final product and morpholin-2-yl methanol were taken and compared to verify signal expressions and their similarity.

Because of the structure of morpholin-2-yl methanol (see **Figure 10**), the main signals of interest would be those generated by the alcohol and the hydrogens located on carbons in between the ether, amide, and alcohol groups; however, because of the abundance of hydrogens on carbons in varying proximities to electronegative atoms, the NMR was expected to be somewhat crowded and therefore hard to visualize. Supplementary computations of the amine NMR suggested that most signals would be found in between 2.5 and 4.0 ppm. Comparison of the simulated NMR for the amine (**Figure 11**) and the experimental NMR for the amine (**Figure 13**) indicate that the computational NMR was a good predictor for experimental signals. The only difference between the two spectrums was a uniform downfield shift of approximately 0.3 ppm.

In fact, aside from the signal at 7.25 ppm produced by residual, non-deuterated chloroform, most of the signals of interest overlap in between 2-4 ppm, so the spectrum is more useful in comparing structures rather than being interpreted. However, general observations can be made about the spectrum; the superimposed peak between 2.5 to 3.0 ppm is generated by the hydrogens bound to the carbons on the side opposite of the alcohol functionality (since there are less electronegative atoms to deshield the hydrogens; **H_A, H_B,**

Figure 10), whereas the signals between 3.5 and 4.0 ppm are produced by the hydrogens on the carbons closest to the alcohol (as there are more electronegative functionalities; **H_D, Figure 10**). The ^{1}H NMR spectrum of morpholin-2-yl methanol is shown in **Figure 13**.

As with the NMR for the amine, the spectrum obtained from the product was expected to be complicated due to the structure of the porphyrin and the number of hydrogen atoms spread across the molecule. An analysis of the molecular structure

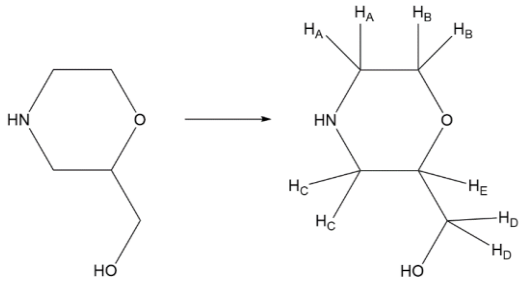

Figure 10: The expanded structure of morpholin-2-yl methanol with hydrogens shown for clarity.

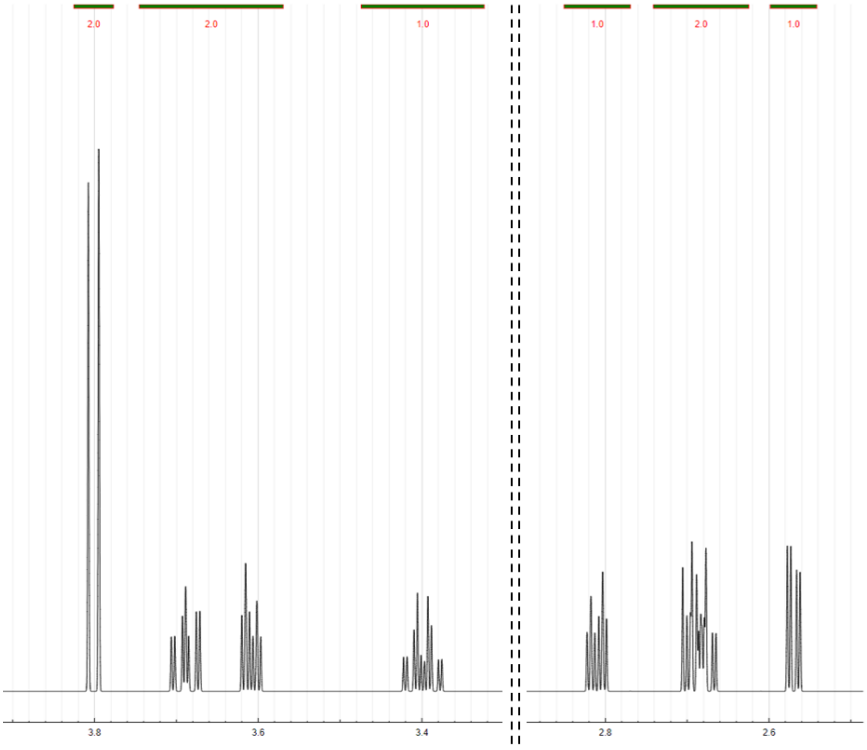

Figure 11: The simulated NMR spectrum of morpholin-2-yl methanol.[17,18] This NMR was simulated using *nmrdb.org* at 600 MHz, a line width of 1 Hz, and 256k data points.

suggested that there should be several superimposed signals greater than 6 ppm since there are hydrogens bound to the pyrrole rings, hydrogens bound to the interior of the porphyrin core, and hydrogens bound to the **benzene** rings in the periphery. Simplified versions of these molecular environments are located at or above this region, which means that the signal expressions in the NMR of the product should be shifted even further downfield. Although two sets of doublets are visualized in this region (7.4 and 8.2 ppm), many of the theoretical signals are missing. Supplementary computations of the porphyrin NMR suggested that one signal would be found around 9.25 ppm consequent of the hydrogens located in the space between the outer core and the aromatic rings in the periphery, along with several other signals between 8.2 and 8.75 ppm (**Figure 12**).

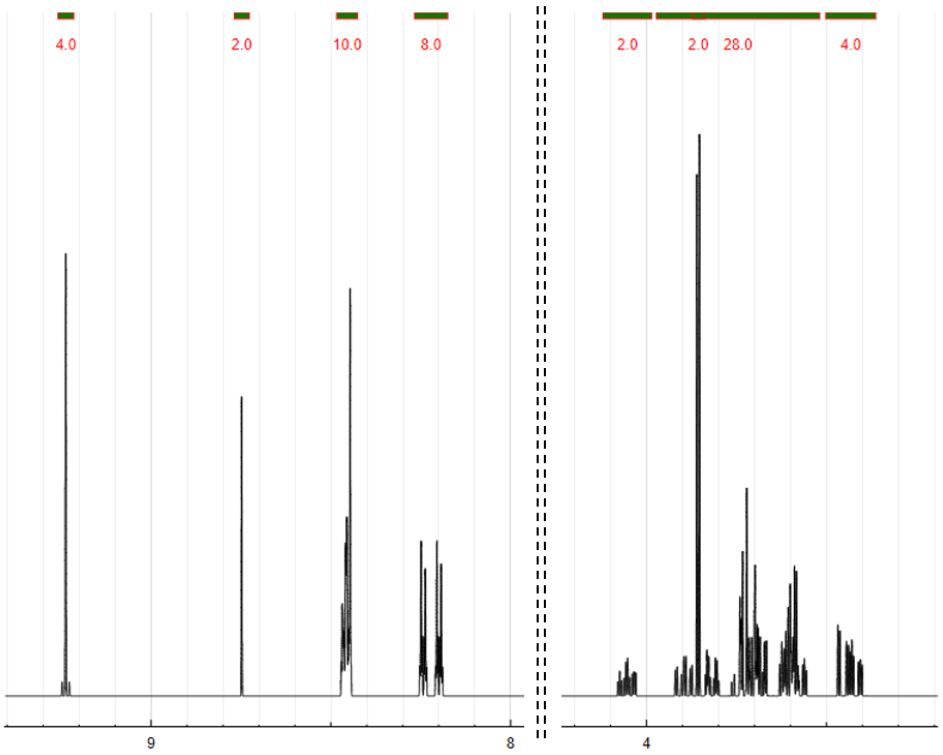

Figure 12: The simulated NMR spectrum of H_2TPP-MorphMeOH.[17,18] The dashed line delineates a split where a portion of the graph containing no signals was removed. This NMR was simulated using *nmrdb.org* at 600 MHz, a line width of 1 Hz, and 256k data points.

The differences between the computational and experimental NMR for H_2TPP-MorphMeOH were twofold. Firstly, the computational NMR displayed herein is purely a simulation. It was expected that the computational and experimental spectra would not match perfectly due to simplifications and mathematical roundoff. Secondly, the simulation failed to consider solvent effects[17]; the NMR product sample was made up in deuterated water, which often causes problems when performing NMR analyses. Most often, deuterated water can exchange protons for deuterium, which can cause peak silencing or shifting since deuterium does not produce NMR signals (the program used to simulate NMR spectrums, *nmrdb.org*, does not predict the signals for protons that are susceptible to interchange, such as those on alcohols, carboxylic acids, etc.).[17] Aside from producing signal offsets, D_2O also tampers with the integration technique used in NMR; the area underneath each peak is calculated and correlated to hydrogens in an attempt to identify each peak, but water tends to skew data somewhat, therefore undermining the procedure (this interference is the reason that peak integration is not used in this analysis).

Although the simulated NMR and experimental NMR don't match perfectly, the product was understood to have been synthesized properly. First, the large peak near 4.7 ppm corresponded to residual non-deuterated water in solution. Next, the sets of doublets visualized at 7.4 and 8.2 ppm were indicative of hydrogen coupling on the benzene rings in the periphery, along with the hydrogens from the pyrrole rings on the exterior of the porphyrin core. Finally, the general shape of the product's upfield NMR is very similar to the shape of the amine's upfield NMR; this, combined with the information concluded from the other analytical techniques, indicates that the product was synthesized properly with the amine coupling to the porphyrin backbone efficiently. The ^{1}H NMR spectrum of both morpholin-2-yl methanol and H_2TPP-MorphMeOH is shown in **Figure 13**.

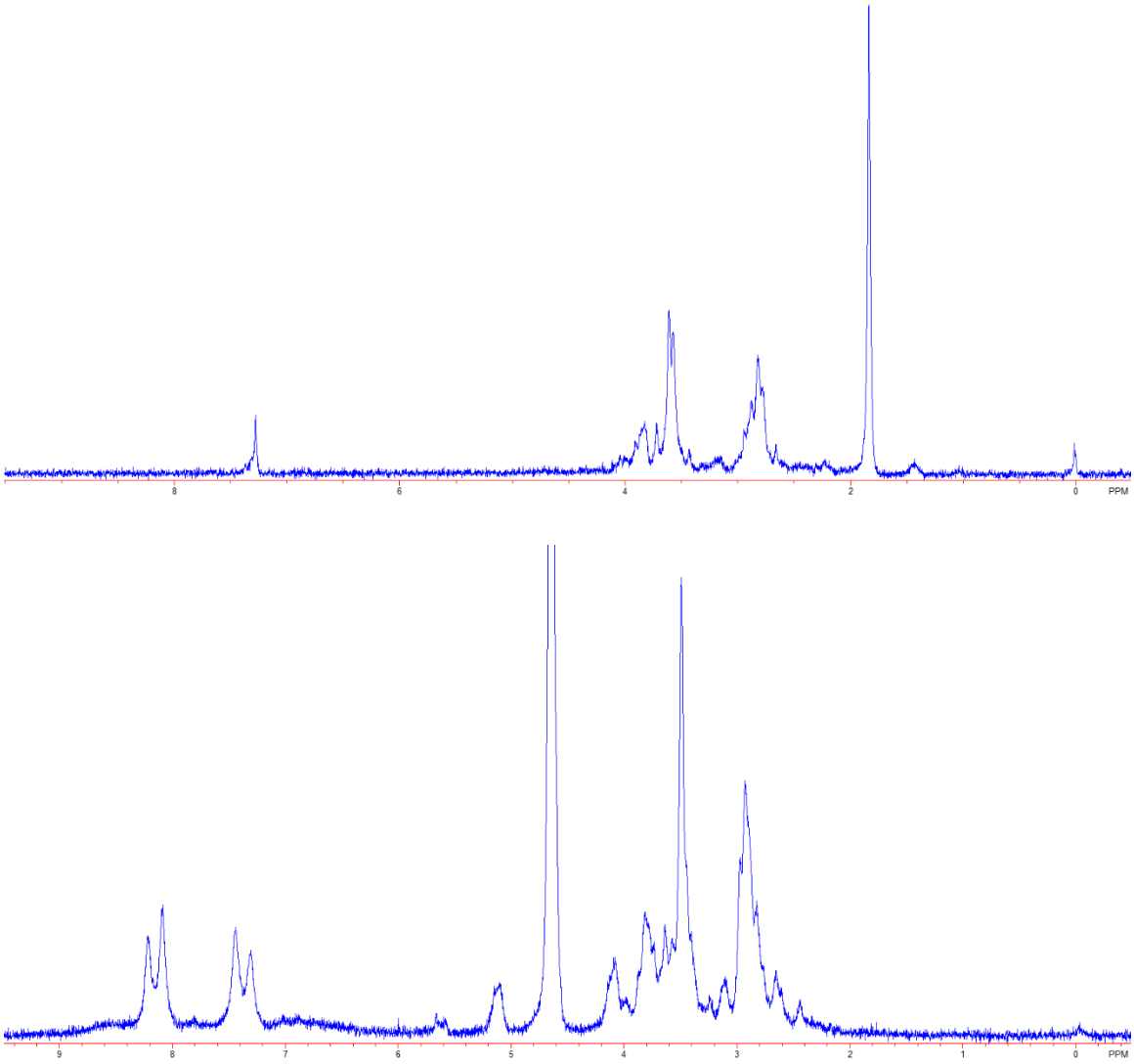

Figure 13: The NMR spectra of the amine, morpholin-2-yl methanol, dissolved in deuterated chloroform ($CDCl_3$) (top), and the product, H_2TPP-MorphMeOH, dissolved in deuterated water (D_2O) (bottom). To get good definition on the product NMR, the tallest peak had to be cut off; the peak extends about ten times higher than that of the tallest peak fully visible in the image of the NMR.

Ultraviolet-Visible (UV-Vis) Spectroscopy

The ultraviolet-visible spectrophotometer used in this research was a Hewlett-Packard 8453 Chemstation recording spectrophotometer with UV-Visible Chemstation software. The cuvette used was a 1 cm × 1 cm quartz cuvette, and the spectrum was run with H_2O as the solvent. UV-Vis spectroscopy was used to calculate the **molar absorptivity coefficients** of the compound at its absorption wavelengths; these values are critical in the calculation of concentrations for subsequent biological assays.

In UV-Vis spectroscopy, a liquid sample is placed into a cuvette made of a transparent material; cheaper cuvettes are made from plastic or glass, which is subject to light scattering and therefore produces a less accurate reading, whereas more expensive cuvettes are made of quartz, which does not absorb in the ultraviolet region (200-350 **nano**meters (nm)). The cuvette is placed into the instrument and the sample is bombarded with wavelengths of light ranging from around 180 to 780 nm, which spans the ultraviolet and visible light range of the electromagnetic spectrum. As the light passes through the sample, the instrument measures the transmittance of each wavelength (ratio of incoming to outgoing intensity).[19] **Figure 14** shows a simplified diagram detailing how UV-Vis spectroscopy works.

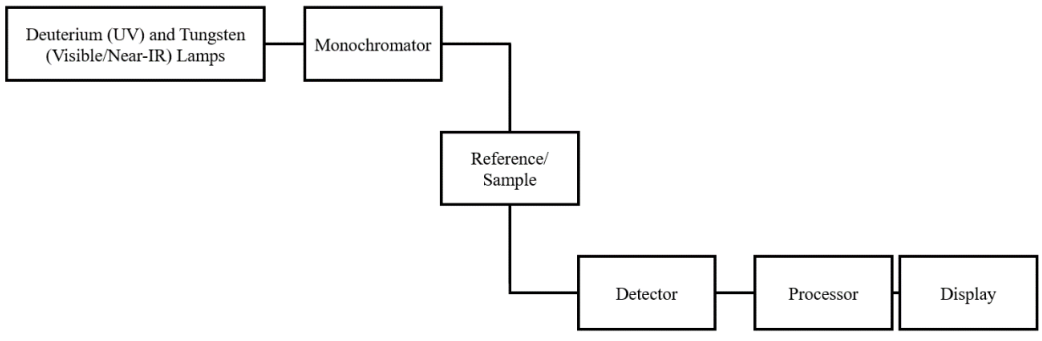

Figure 14: A simplified diagram showing how UV-Vis spectroscopy works. Although depicted as two 90º turns in the diagram, the entire apparatus is normally in a straight line from the lamps to the detector.

The relationship between the absorbance of light and the concentration of a singular species is defined by the Beer-Lambert law:

$$A = \varepsilon c l$$

where A is the absorbance (which is unitless), ε is the molar absorptivity coefficient (traditionally having units of $M^{-1}cm^{-1}$), and l is the path length of the compound (i.e., how far the light travelled through the species during the analysis, traditionally having units of centimeters). As established by this relationship, species with higher absorptivity coefficients produce absorptions greater than species with lower coefficients, provided that the path length is equivalent.[19]

To accurately determine the product's molar absorptivity coefficient, several analytes were prepared in differing concentrations and measured to develop a calibration curve. By plotting the absorbances as functions of the concentrations in the form of a scatter plot and extrapolating the best-fit line, a more reliable value for the coefficient was determined, rather than one calculated from a single measurement; additionally, developing this curve allowed for a degree of error to be measured and reported for the coefficient.

When porphyrins undergo UV-Vis analysis, two characteristic regions known as the Soret band and the Q bands appear in the UV-Vis spectrum due to specific excitations in the molecule. The Soret band corresponds to an electron dipole moment that relates to energy level transitions and is the most intense peak in the spectrum, while the Q bands correspond to vibrational activity and are much less pronounced.[20] In porphyrins, the Soret band typically manifests between 400-450 nm with an absorptivity coefficient on the order of 100 $cm^{-1}mM^{-1}$ and the Q bands between 500-600 nm with an absorptivity coefficient on

the order of 1 $cm^{-1}mM^{-1}$. Because the final product was a porphyrin derivative, these regions were expected in the UV-Vis spectrum around their associated wavelengths.

As shown in **Figure 15**, the molar absorptivity coefficient for the Soret band (413 nm) is in the anticipated range, whereas the molar absorptivity coefficients for the peaks in the Q bands are lower than expected; however, beyond mere observation, this characteristic has no immediate implications for the utility of H_2TPP-MorphMeOH. The molar absorptivity coefficient is later used to calculate compound concentrations in the cell metabolic assay, and if the compound were to be found as a potential phototherapy agent, the lower absorptivity in the Q bands would mean that the light used for photoactivation would need to be more intense.

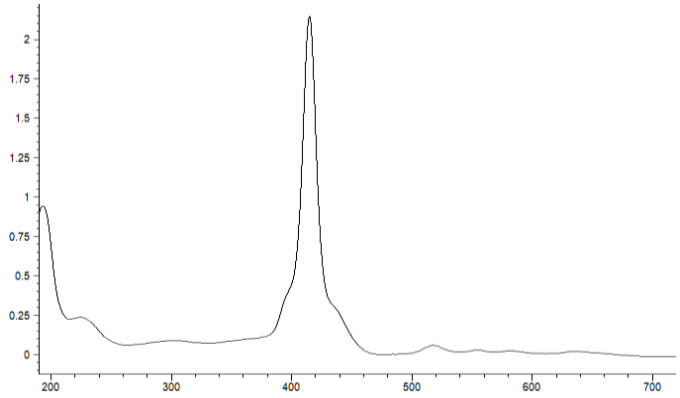

Figure 15: The UV-Vis spectrum of the product, H_2TPP-MorphMeOH, in H_2O. The x-axis has units of nanometers and the y-axis is the solution absorbance, which is unitless.

Peaks (nm)	**Molar Absorptivity Coefficient, ε ($cm^{-1}mM^{-1}$)**
413	120
518	5.35
555	2.93
581	2.45
636	1.95

Table 1: A list of the molar absorptivity coefficients for H_2TPP-MorphMeOH.

High-Performance Liquid Chromatography (HPLC)

Upon verifying the structure of H_2TPP-MorphMeOH, High-Performance Liquid Chromatography (HPLC) was used to determine the purity of the compound. The HPLC instrument used was a Waters e2695 Separations Module with Waters 2996 Photodiode Array Detector. The column and flow rate used for analysis were a Nova-Pak C_{18} 3.9 × 150 mm HPLC column using acetonitrile as the eluent with a flow rate of 1 mL/min and a detection wavelength of 254 nanometers (nm).

In HPLC, a liquid sample is prepared from a compound and the chosen solvent, known as the mobile phase, or the part of the analytical system that moves. This solution is pumped into a column filled with chromatographic material known as the stationary phase, or the part of the system that doesn't move, at high pressures (often several thousand pounds per square inch). To mediate the separation, the sample is passed through the column by an inert carrier liquid (the solvent), such as acetonitrile. To identify components in the mixture and determine the purity of the sample, a property known as the retention time is analyzed; the retention time is defined as the length of time it takes for a component to exit the column. This time is determined by the interactions between the component and the two phases; components that have the least interaction with the stationary phase or the most with the mobile phase will exit the column faster, and vice versa. This interaction is usually the result of polarity differences, where one phase is nonpolar and the other is polar.[21] In the case of this research, the HPLC was performed using reverse phase chromatography, in which the stationary phase was nonpolar, and the mobile phase was polar. The stationary phase used was C_{18}, which is made from octadecylsilane, (a long chain of single-bonded hydrocarbons attached to a silicon atom) while the mobile phase

was acetonitrile (one hydrocarbon bound to a carbon that is triple-bonded to a nitrogen). **Figure 16** shows a simplified diagram detailing how HPLC works.

To determine the purity of an analyte, the area underneath the curve of interest is determined. The area under the peak of interest divided by the total area underneath all of the peaks is a decimal representation of the purity of the sample, which can then be multiplied by 100 to give a percent purity of the sample.

In the case of H_2TPP-MorphMeOH, the area under the peak of interest comprised 98% of the area under all of the chromatogram peaks, so the purity of the sample was determined to be 98%. Additionally, the retention time range for the product was determined to be 1.29 minutes. **Figure 17** shows an image of the HPLC chromatogram for H_2TPP-MorphMeOH.

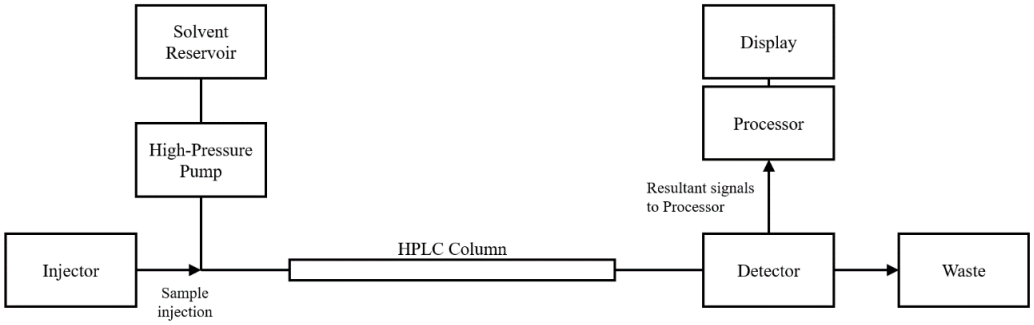

Figure 16: A simplified diagram showing how HPLC works.

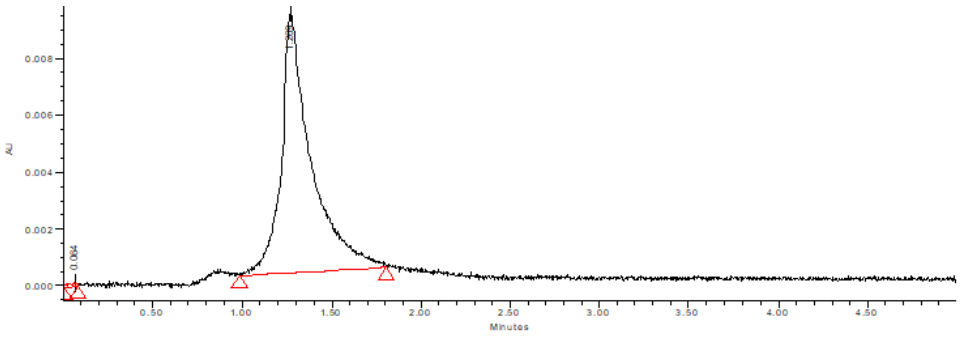

Figure 17: The HPLC chromatogram of the product, H_2TPP-MorphMeOH.

Cytotoxicity Testing

Once the final product was purified and characterized, a biological assay called an MTT assay was performed to determine if H_2TPP-MorphMeOH would work as a photodynamic therapy agent. The premise of the assay is to experimentally determine the correlation between the concentration of the compound and its cytotoxic strength, then draw a conclusion of its potential utility based on the observed **LD_{50}**. In general, lower LD_{50} values for light-exposed plates indicate a more cytotoxic compound.

To perform the assay, a series of controls and concentrations of H_2TPP-MorphMeOH were applied to two plates containing TNBC cells. One plate was kept in darkness to monitor the porphyrin's effect on TNBC cells in the dark and to act as a control for the experiment, while the other plate was exposed to a specific quantity of light to produce the ROS that induce cell apoptosis. A viable PDT agent will exhibit little cytotoxicity when not exposed to light and will exhibit high cytotoxicity once exposed to light.

Preparation

In preparation for the MTT Assay, MDA-MB-231 triple-negative breast cancer cells were cultured by Alexander Podguzov and Dr. Timothy Hayes in the cell growth medium recommended by the **American Type Culture Collection (ATCC).** The cells were plated onto two 96-well plates in the concentration of 1000 cells per square centimeter and were incubated at 37 °C. Additionally, samples of the experimental compound were prepared in varying concentrations (0 – 100 micro**molar** (μ**M**)) in cell growth medium.

To start, two microfuge tubes were prepared with 3-5 mg of the compound and the appropriate amount of solvent to produce 0.030 M solutions. These would serve as the stock solutions for the production of subsequent concentrations. Using the molar absorptivity coefficient calculated during the characterization of the compound, the actual concentration of each stock sample was calculated via an anticipated mathematical dilution (a sample with an absorbance of 1), then comparing it to the actual absorbance value. For example, if the dilution was from 0.03 M to 0.003 M to produce an absorbance of 1, and the actual absorbance was 1.5, it follows that the concentration of the diluted sample was actually 0.0045 M and the stock concentration was 0.045 M.

Using the updated concentrations for each microfuge tube, calculations were performed to prepare 2 mL dilutions of 1, 3, 10, 30 and 100 μM in cell growth medium to be plated on the cells. In practice, this range of concentrations is a good start towards determining the cytotoxic efficacy of the compound.

However, because the difference between the stock concentration and the plating concentrations was several orders of magnitude (between 10^2-10^4 times), producing serial dilutions directly from the stock was impossible. For example, performing dilutions to the lower plating concentrations in this fashion would require aliquots with volumes less than 1 μL; attempting to do so would lead to severe problems in accuracy, as this is the lower physical limit for measuring reliable volumes. Instead, intermediary "working" stocks were created to bridge the gap. This was accomplished by calculating the volumes of the working stock needed for plating, then determining an appropriate intermediate concentration. However, before the calculations to prepare the intermediates were performed, there was one more restriction to be considered.

Because the stock sample and working samples were created using dimethyl sulfoxide (DMSO) as the solvent, care was taken to minimize the final volume of DMSO that would be applied to the plate. Dimethyl sulfoxide is a widely used industrial solvent that can dissolve both polar and nonpolar compounds and is also miscible in water. For this reason, DMSO is an ideal solvent for cell metabolic assays. However, exposing cells to DMSO in large concentrations (>0.5% v/v) can cause adverse cytotoxic effects.[22] The general rule for preparing plating samples was to keep the final volume of DMSO in each plating concentration (2 mL) to less than 10 μL (0.5% v/v); nevertheless, to rule out any potential influence on cell survival, a control using 10 μL of DMSO was also plated.

Approximately 72 hours after cell plating, the experimental compound was applied to the plates in the aforementioned concentrations. First, using the dilution calculations, two milliliters of each plating concentration were prepared from the stocks and two milliliters of the media. Next, the old media on the cells was aspirated; then, using a micropipet, the samples and controls were added to the cells. On both plates, each control and plating concentration was added to eight replicate wells containing 100 microliters of media. Finally, with the plates now containing the photosensitive agent, both were wrapped in aluminum foil to limit exposure to light. From this point forward, the treated plates were handled in reduced or indirect light.

Eighteen to twenty-four hours after porphyrin application, the cell culture medium was removed and replaced with untreated medium on both plates and the “light” plate (that is, the plate designated for light exposure) was exposed to white light for 17 minutes at an intensity of 0.5 joules per square centimeter to “activate” the applied compound. Following this light exposure, both plates were placed back into the incubator.

MTT Assay

Three days after light exposure, both the "light" and "dark" (that is, the plate not designated for light exposure) plates were removed from incubation and subjected to an MTT assay to determine the cytotoxic efficacy of the experimental compound.

The MTT assay is a colorimetric assay used to measure cell metabolic activity[23]; under specific conditions, this assay can be used to quantify the number of viable cells present in a sample. Enzymes produced by an active cell line can reduce MTT to an insoluble formazan, which has a distinct purple color.[24] Using a spectrophotometer, a relationship between the intensity of the purple color and the presence of working mitochondria can be drawn.[25] **Figure 18** shows the reaction by which MTT is reduced into a formazan, and the purple formazan produced on a plate treated with H_2TPP-MorphMeOH and exposed to light is shown in **Figure 19**.

The spectrophotometer used to perform the MTT assay was a Tecan Infinite M200 with a measurement wavelength set to 570 nm and a corrective wavelength set to 630 nm. After performing the first MTT assay and interpreting the data, a second microplate was prepared using the same procedure but with different concentrations of the compound;

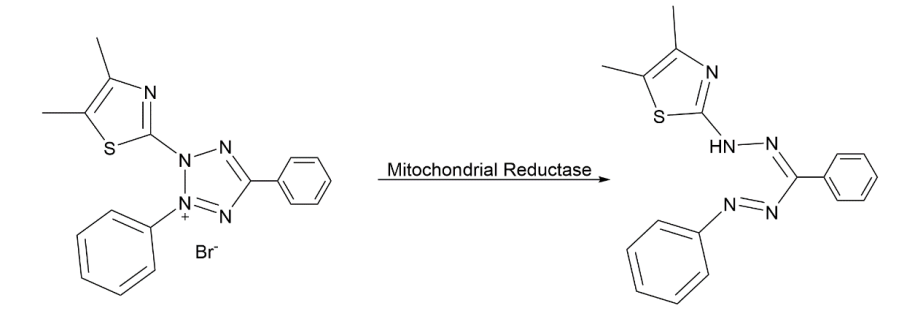

Figure 18: The reaction between MTT and mitochondrial reductase that results in a colored formazan.

Figure 19: A microplate treated with the experimental compound and exposed to light. The five columns of wells on the right contain the various concentrations of H_2TPP-MorphMeOH.

using the cytotoxicity results of the first MTT assay as a guide, a new set of concentrations were chosen to better gauge the compound's cytotoxic effect. If in the first assay the porphyrin was stronger or weaker than the starting concentrations could accurately report, the second assay would use a set of concentrations near the anticipated effective concentration. The plating concentrations for the second assay were chosen based on the cytotoxicity trend present in the first assay.

MTT Data Analysis and Results

Data retrieved from the spectrophotometer during the MTT analysis described only the color intensity within each of the wells on the plate – without modification, the results did not directly describe the viability of the treated cells and, by extension, the efficacy of H_2TPP-MorphMeOH. Conclusions about H_2TPP-MorphMeOH would instead be made from a graph of percent viability versus porphyrin concentration. To determine this information, the raw data needed conversion. First, the absorbance data was imported from the spectrophotometer into an analysis software; in this software, the absorbances for each set of eight replicate control wells and each set of eight replicate treated wells were averaged. Dixon's Q-Test at a 90% confidence interval was then used to filter outliers from the data. Next, each absorbance was converted into a percent viability; this was done by dividing the absorbance by the average absorbance of the untreated wells. After plotting the results in the form of a scatter plot, error bars were added using the standard deviation of each set of replicate wells.

Compounds that are considered strong and viable anticancer PDT agents initially satisfy two conditions. First, the compound is able to kill the exposed cells in very low concentrations, and second, the compound does nothing to the cells that remain unexposed to light. Specifically, the compound should have next to no effect on cell viability in "dark" conditions and the compound should be able to exert its full effect before the ideal LD_{50} threshold – approximately 10 μM – in "light" conditions.

It was concluded from the results of the first MTT assay that the compound was not a strong antineoplastic agent; that is, H_2TPP-MorphMeOH was not found to be effective in inhibiting the growth of TNBC. Even at 100 μM, the highest of the plating

concentrations, the viability of the treated cells was still around 60%. Additionally, it was also inferred that the compound did have a mild cytotoxic effect on the cells not exposed to light, as the average viability across all "dark" concentrations was around 80-85%. **Figure 20** shows the graph of viability versus concentration for the first MTT assay.

Using the data trend, the LD_{50} was estimated to be 140 µM. From this information, a second MTT assay was performed using concentrations of 50, 100, 150, 200, and 250 µM, which would provide significant margins around the first LD_{50} determination to better quantify the true LD_{50}.

It was concluded from the results of the second MTT assay that the compound was, under the conditions of exposure, not a strong antineoplastic agent toward MDA-MB-231 triple-negative breast cancer cells. Although there was significant fluctuation in both the percentage viabilities in both the exposed and unexposed plates, the relationship between the compound concentration and observed cytotoxicity was still present. Using this data, the *in vitro* LD_{50} of H_2TPP-MorphMeOH was estimated to be 120 µM. **Figure 20** shows a graph of viability versus concentration for the second MTT assay.

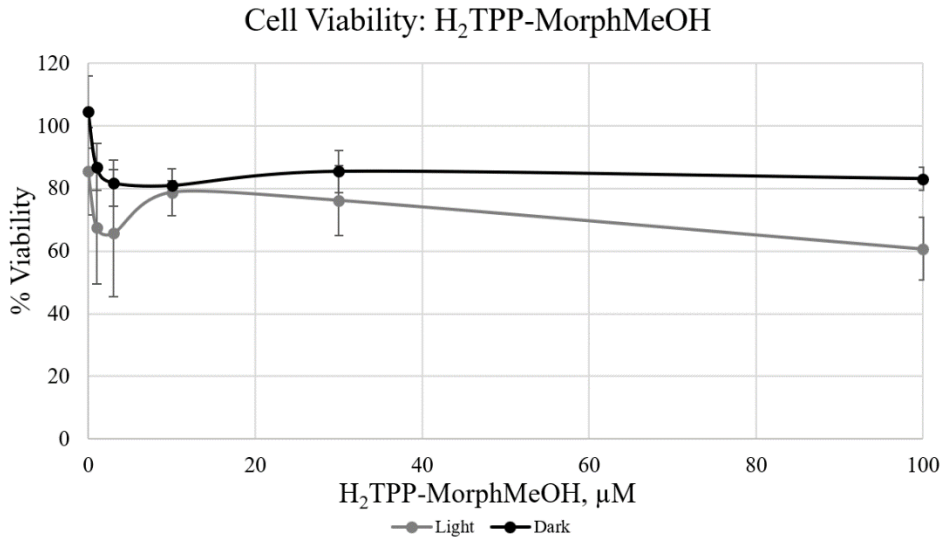

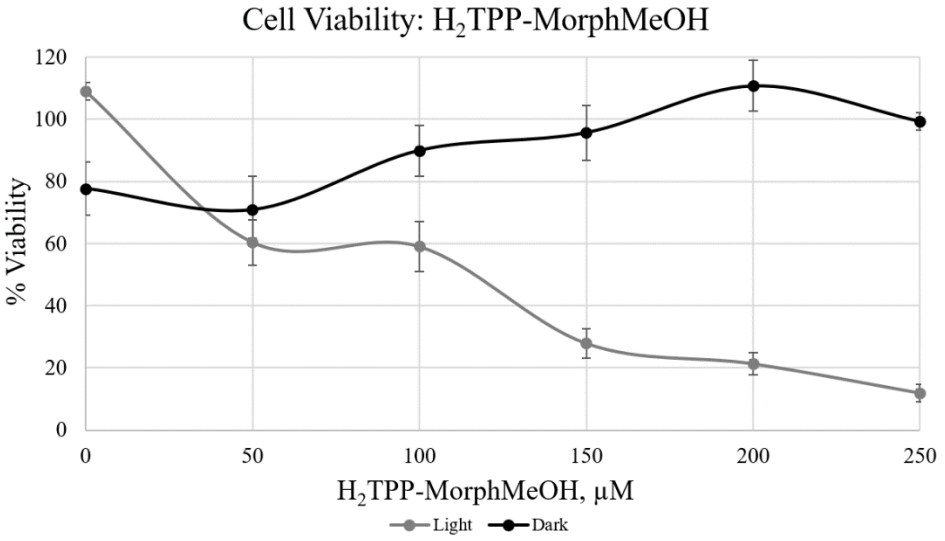

Figure 20: The results of the first (top) and second (bottom) MTT assays using H_2TPP-MorphMeOH.

Conclusions

As mentioned earlier, this research intended to synthesize a novel, water-soluble porphyrin with strong anticancer characteristics. Based on the results from the instrumental analysis, it was concluded that the proposed reaction was successful in producing a novel, water-soluble porphyrin with confirmed structure and purity, but the results of the MTT analysis revealed that the compound was not a strong anticancer agent toward MDA-MB-231 triple-negative breast cancer cells and was therefore not a candidate for photodynamic therapy for this type of cancer.

In the synthesis, the reaction yield was calculated to be 6.8%, which was low but still acceptable for a condensation synthesis under these experimental conditions. Following the purification, the results from the HPLC indicated that the product was 98% pure. Based on the results from the IR and NMR analyses, it was concluded that the amine was successfully bound to the porphyrin core and that H_2TPP-MorphMeOH was produced as intended. Finally, the outcomes of the MTT analyses revealed that the product did not exhibit strong cytotoxic characteristics for this cell line, as the estimated LD_{50} was 120 µM, over ten times weaker than desired.

Even if follow up tests are performed to refine experimental details (for example, a follow-up MTT using the concentrations plated for the second analysis to resolve any data errors), H_2TPP-MorphMeOH is not expected to display a response that would justify its use as an antineoplastic agent. Despite this lack of success, the product may show potential against other cell lines or in another field of research and development. As it is a porphyrin, H_2TPP-MorphMeOH may possess characteristics that permit its use in other medicinal endeavors, or potentially as an organic dye in sensitized solar cell development.

The Future of Porphyrin Chemistry

As stated earlier, the complexity of porphyrins gives them significant utility. Armed with the conclusions drawn from the analyses conducted on H_2TPP-MorphMeOH, the potential applications of this porphyrin in other fields of research should be considered.

Medicinal Applications

To date, several porphyrin derivatives have already been approved for use in the treatment of various cancers. Photofrin (porfimer sodium) was the first photodynamic therapy agent approved for cancer treatment in 1995[26]; although first used for the treatment of obstructive esophageal cancer, its use was later expanded to include treatment for lung, bladder, and cervical cancers, amongst others.[27] Since this development, several more "second generation" photosensitizers have been approved for treatment, including temoporfin (Foscan), verteporfin (Visudyne), and talaporfin (Laserphyrin) (**Figure 21**). Currently, research and clinical development is oriented in the direction of producing "third generation" photosensitizers via novel synthesis that will improve upon cancer-targeting efficiency, cytotoxic efficacy, and systemic delivery.[28] As stated previously, however, H_2TPP-MorphMeOH is not a strong cytotoxic agent against the MDA-MB-231 cell line and appears to not be a prime candidate for photodynamic therapy in general.

Aside from PDT, porphyrin derivatives may also display alternative biological capabilities. Although not employed commercially, some porphyrin derivatives have been studied as catalysts for organic compound oxidations; some derivatives can catalyze synthetic reactions or emulate the action of various biological enzymes when complexed

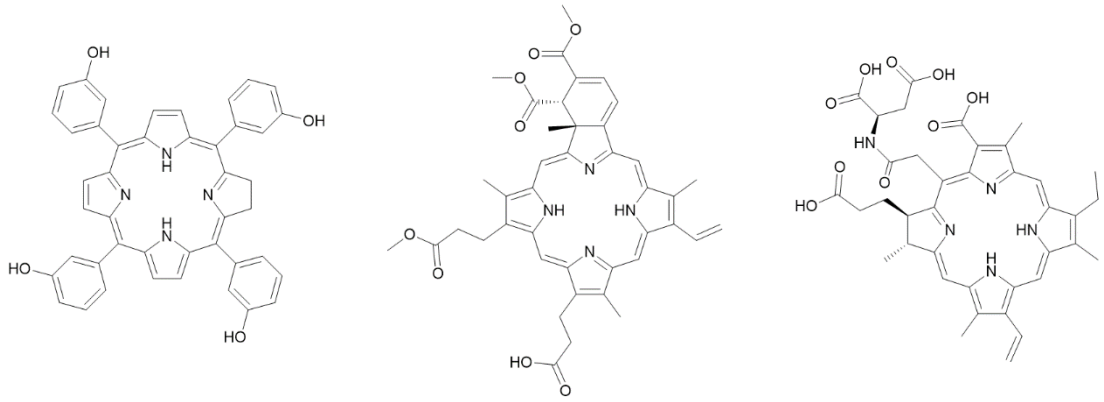

Figure 21: Structures of porphyrins currently used in the treatment of cancers. From left: temoporfin, verteporfin, and talaporfin.[28,29]

with a metal such as manganese, iron, or cobalt.[30] In addition to biomimetic catalysis, porphyrins have also been used in wound healing and monitoring. In 2014, an oxygen-sensing porphyrin phosphor was integrated into a liquid bandage matrix to produce a system that could monitor cutaneous oxygenation via the porphyrin's phosphorescence; this development could act as an aid to addressing poor wound healing and costly chronic wound recurrence due to poor oxygenation.[31]

Because H_2TPP-MorphMeOH is an organic porphyrin, it lacks the metal element required for operation as a biomimetic catalyst. However, as the oxygen sensitivity and the phosphorescent capacity of H_2TPP-MorphMeOH have never been analyzed, it may be suitable for wound healing, although its non-negligible cytotoxic effects may prove counterproductive.

Solar Cell (Photovoltaic) Applications

Concerns of widespread global warming in the last two decades has kickstarted research towards alternative energy sources such as geothermal, hydroelectric, and wind power; however, one of the most promising alternative sources is photovoltaics, or the

harnessing of solar energy. With the sun supplying the Earth over 10^{17} W (a hundred quadrillion watts), harnessing even a fraction of this would be more than enough to satisfy humanities' energy needs.[32]

The main way this energy is harnessed is through solar cells, which are traditionally comprised of a semiconductive compound such as silicon dioxide (SiO_2) doped with electron sufficient and deficient elements (phosphorous and boron, respectively). With an energy efficiency of up to 16%, a working lifetime exceeding 20 years, and a simple electron system for producing electricity (**Figure 22**), these cells have been considered the workhorse of the PV industry for years.[32] However, recent research has been devoted to the development of alternative solar cell types, such as thin-film and dye sensitized solar cells that increase efficiency or reduce production costs.[33] H_2TPP-MorphMeOH may possess characteristics that allow it to act as a dye in dye-sensitized solar cells.

Dye-sensitized solar cells (DSSCs) are different from traditional silicon cells in that the electrical production process requires more internal steps and materials (**Figure 23**) in

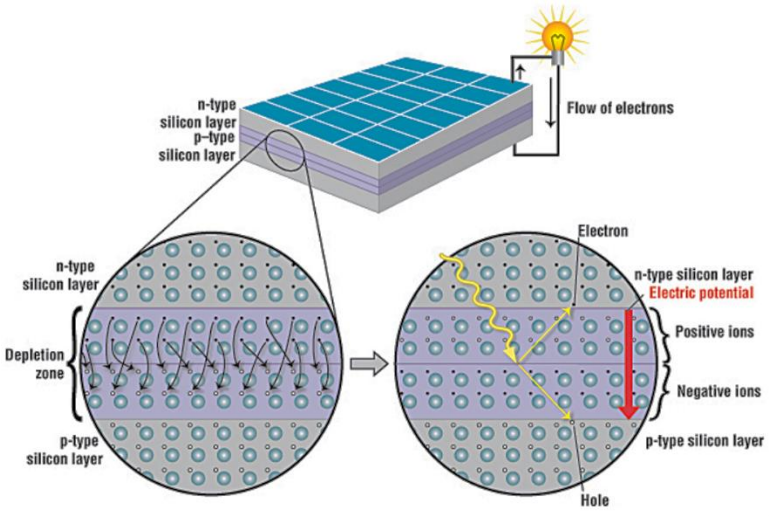

Figure 22: A diagram of a silicon-based solar cell.[34] Sunlight enters the cell and excites an electron from the n-type silicon (electron surplus) to the p-type silicon (electron deficient), which produces a current when the two electrodes are connected.

exchange for lower production costs and more efficient electricity production. Instead of two doped semiconducting regions as in a silicon cell, a DSSC uses a semiconductive compound sensitized with a dye and an electrolyte system.[35]

Traditionally, DSSCs use titanium dioxide, or TiO_2, as the semiconductor in the cell. However, TiO_2 alone is not enough to yield high efficiencies from a solar cell; the amount of energy required to dislodge an electron from the semiconducting molecule and produce a current is known as the bandgap of the compound, and the bandgap of titanium dioxide is disadvantageously large. To produce a current from unmodified titanium dioxide, incident light must be in the ultraviolet (UV) range (<~388 nm), meaning that a solar cell semiconductor comprised solely from TiO_2 would be practically useless, as less than 5% of light incident on Earth's surface is comprised of UV light. To make up for this disadvantage, a sensitizer is added to the solar cell; a sensitizer is a compound that has a ground energy level higher than that of ground level TiO_2, but less than its excited state.

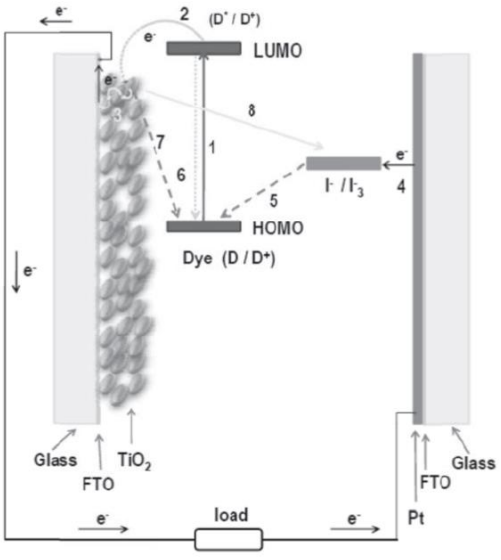

Figure 23: A diagram of a dye-sensitized solar cell.[35] Notice that the electron schematic is more complex. There are more competing actions in this cycle than the ones in traditional solar cells; steps 1, 2, 4, and 5 make up the ideal electron cycle, whereas steps 3 (within TiO_2 near top of diagram), 6, and 7 show competing steps.

This way, light of longer wavelengths can dislodge electrons from the dye into the semiconductor to produce electricity, thus increasing the solar cell's utility.[36] **Figure 24** shows the electron transport mechanism that DSSC's rely on to produce electricity from sunlight.

Despite requiring more individual materials for its assembly, DSSCs ultimately require less amounts of each material and therefore cost less; additionally, DSSCs are better at dissipating heat, which contributes to a lower operating temperature and higher efficiency. The only drawback that current research intends to resolve is DSSC's shorter working lifespan and sensitivity to air which, until this issue is resolved, can be mediated by vacuum sealing of the cells.[35]

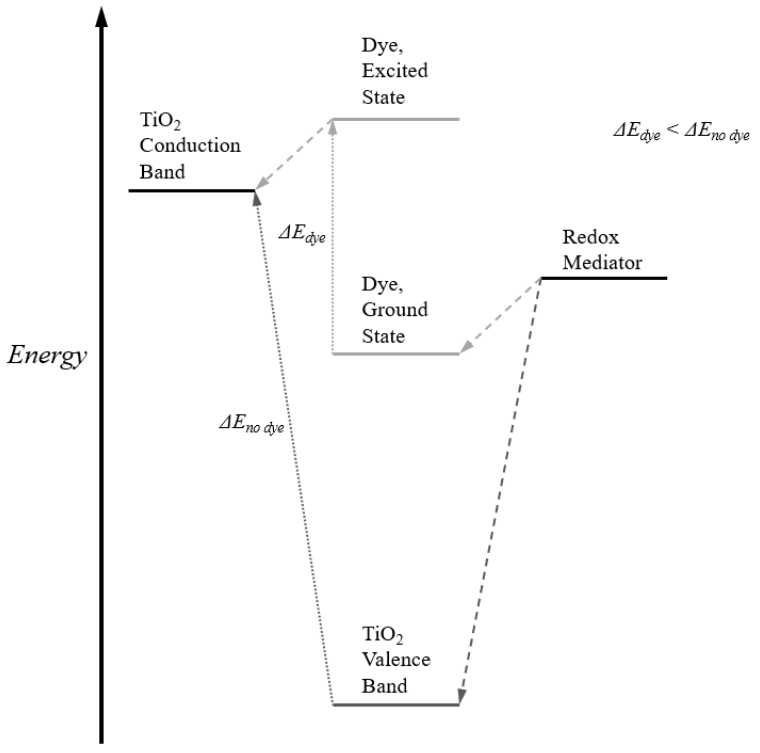

Figure 24: A simplified diagram of electron excitation in a dye-sensitized solar cell. In general, lower energy requirements (ΔE) correspond to better performance. The introduction of a dye prevents the need to excite an electron from the lowest possible energy state, meaning that more wavelengths of light can be used for excitation and a greater percentage of incident light can be harvested.

Although research into different semiconducting compounds has been performed, titanium dioxide remains the most commonly employed semiconductor for DSSCs; similarly, research into different electrolyte systems has been performed, but the iodine-triiodide system remains the most common (although cobalt-based electrolytic systems are becoming more common). Therefore, improvement of these solar cells stems predominately from the optimization of the sensitizers.[37]

Originally, dyes were formed from a type of metal complex (often ruthenium-based) that possessed significant electron density through conjugated molecular systems. About a decade after the first DSSC was produced, investigations into utilizing porphyrin-based dyes began; since, porphyrins have continually been of significant interest because of a closely related, natural process of light harvesting. Chlorophylls, which perform the light absorption process in plants, are a metalloporphyrin derivative. As biological systems based around chlorophyll would suggest, porphyrins possess an electron-dense system that, under the proper conditions, can participate in the efficient conversion of energy.[38]

Typical structures for porphyrin dyes involve three significant regions: a donor moiety, an electron bridge system, and an acceptor/anchor moiety. The donor moiety is responsible for the electron excitation from sunlight, as it has a surplus of electrons and can efficiently transmit them through the solar cell. The electron bridge system is the core of the dye which links the donor and acceptor regions and possesses a conjugated bond system which excited electrons can use to travel between the donor and the acceptor regions. Finally, the acceptor/anchor moiety serves two purposes; first, it anchors the dye to the titanium oxide layer so that electrons can be passed through the solar cell, and second, the moiety accepts excited electrons and passes them into the conduction band of the

semiconducting layer.[38] However, research has progressed to the point that the structure of the dye itself is being revitalized, as recent breakthroughs in efficiency suggest that more internal functionalities increase the efficiency of the dye. The greatest change arises from the optimization of the anchor moiety, where newer-generation dyes rely on the juxtaposition of an electron deficient and electron rich unit to fuel a "push and pull" system for charge transfer; since this structure was published, efficiencies of solar cells produced with novel dyes have nearly doubled.[39] The general structure for push-pull porphyrins is shown in **Figure 25**.

Regarding the potential utility of H_2TPP-MorphMeOH, it is believed that the porphyrin would not prove useful in dye-sensitized photovoltaics as the primary dye. The majority of current porphyrin based DSSC technology and research focuses on the use of metalloporphyrins, or porphyrins that are combined with a metal (such as heme). Because H_2TPP-MorphMeOH is an organic porphyrin, it is unclear if it would be useful in DSSC development. However, structurally, H_2TPP-MorphMeOH is incompatible as it is. The structure of H_2TPP-MorphMeOH lacks all of the prerequisite structures for a porphyrin dye (with the exception of the porphyrin core itself); without an anchor, it cannot adsorb onto the titanium dioxide surface, and without a donor, it cannot transfer electrons. Modifying the structure would result in the creation of a new compound, so H_2TPP-MorphMeOH cannot be the primary dye in a DSSC.

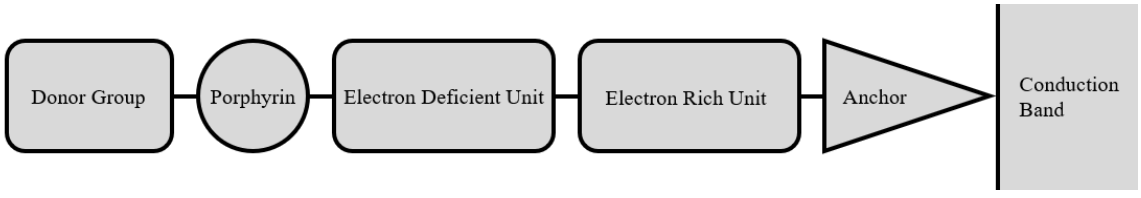

Figure 25: A generalized diagram of the structure of push-pull porphyrins. Incident light excites an electron at the donor moiety, which then migrates across the molecule and into the conduction band via conjugated pi bonds.

As identified in the UV-Vis analysis of H_2TPP-MorphMeOH, porphyrins used as dyes in DSSCs still suffer from one significant flaw that must be considered during the production of these solar cells. Porphyrins exhibit significant light absorbing properties around the Soret band and less so around the Q bands but fail to absorb other wavelengths of light. Just as useable energy would be lost if a solar cell were comprised solely from titanium dioxide, producing a cell from a single porphyrin would result in wavelengths of light lost simply because the dye isn't attuned to those wavelengths. For this reason, the field of solar cosensitization has become more popular. During the creation of a cosensitized cell, a porphyrin dye is adsorbed to the TiO_2, followed by a second organic dye that absorbs light in the areas where the porphyrin doesn't. If the two dyes are compatible, significantly more wavelengths of light can be converted into electricity at greater intensities and the efficiency of the solar cell increases.[40]

However, even though H_2TPP-MorphMeOH is an organic compound, using it as the secondary dye to a DSSC is counterproductive if the primary dye is another porphyrin. Since both possess absorption patterns characteristic of porphyrins, using porphyrins for both the primary and secondary dyes defeat the purpose of cosensitization, so utilizing a secondary dye that is not a porphyrin may potentially prove beneficial. Incorporating a metal into the porphyrin core of H_2TPP-MorphMeOH may increase both its cytotoxicity as a PDT agent and its utility as a dye in DSSC's, but it has been concluded that H_2TPP-MorphMeOH would not be proper for use in either application as of now.

References

1. "Porphyrin." *Encyclopædia Britannica*, Encyclopædia Britannica, Inc., 7 Apr. 2016, www.britannica.com/science/porphyrin.

2. Harper, Douglas. "Porphyrin." *Online Etymology Dictionary*, www.etymonline.com/search?q=porphyrin.

3. Dayan, Franck, and Emilie Dayan. "Porphyrins: One Ring in the Colors of Life." *American Scientist*, Sigma Xi, 2 Feb. 2018, www.americanscientist.org/article/porphyrins-one-ring-in-the-colors-of-life.

4. "Photodynamic Therapy for Cancer." *National Cancer Institute*, National Institutes of Health, 6 Sept. 2011, www.cancer.gov/about-cancer/treatment/types/surgery/photodynamic-fact-sheet.

5. "NCI Dictionary of Cancer Terms." *National Cancer Institute*, National Institutes of Health, www.cancer.gov/publications/dictionaries/cancer-terms/def/reactive-oxygen-species.

6. Ash, Caerwyn, et al. "Effect of Wavelength and Beam Width on Penetration in Light-Tissue Interaction Using Computational Methods." *Lasers in Medical Science*, vol. 32, no. 8, 2017, pp. 1909–1918., doi:10.1007/s10103-017-2317-4.

7. "Getting Photodynamic Therapy." *Radiation Therapy*, American Cancer Society, 2 Mar. 2020, www.cancer.org/treatment/treatments-and-side-effects/treatment-types/radiation/photodynamic-therapy.html.

8. "Triple-Negative Breast Cancer." *Centers for Disease Control and Prevention*, U.S. Department of Health and Human Services, 14 Sept. 2020, www.cdc.gov/cancer/breast/triple-negative.htm.

9. Miller, Eric J., and Sarah L. Lappin. "Physiology, Cellular Receptor." *StatPearls, NCBI*, U.S. National Library of Medicine, 3 May 2020, www.ncbi.nlm.nih.gov/books/NBK554403/.

10. "Step 1: Discovery and Development." *The Drug Development Process*, FDA, 4 Jan. 2018, www.fda.gov/patients/drug-development-process/step-1-discovery-and-development.

11. Reusch, William. *Infrared Spectroscopy*, Michigan State University, 5 May 2013, www2.chemistry.msu.edu/faculty/reusch/VirtTxtJml/Spectrpy/InfraRed/infrared.htm.

12. “Schematics of a Two-Beam Absorption Spectrometer.” *Wikipedia*, 7 Apr. 2011, en.wikipedia.org/wiki/Infrared_spectroscopy#/media/File:IR_spectroscopy_apparatus.svg.

13. “IR Spectrum Table & Chart.” *Millipore Sigma*, Sigma Aldrich, 2020, www.sigmaaldrich.com/technical-documents/articles/biology/ir-spectrum-table.html.

14. Parker, Frank S. “Amides and Amines.” *Applications of Infrared Spectroscopy in Biochemistry, Biology, and Medicine*, 1971, pp. 165–172., doi:10.1007/978-1-4684-1872-9_8.

15. “What Is NMR? Nuclear Magnetic Resonance.” *Bruker*, www.bruker.com/fileadmin/user_upload/8-PDF-Docs/MagneticResonance/NMR/brochures/what-is-nmr_brochure_0115_T153283.pdf.

16. Raja, Pavan M. V., and Andrew R. Barron. “5.3: NMR Spectroscopy.” *Chemistry LibreTexts*, Libretexts, 24 July 2019, chem.libretexts.org/Courses/University_of_Illinois_Springfield/Introduction_to_Organic_Spectroscopy/5:_Proton_Nuclear_Magnetic_Resonance_Spectroscopy_(NMR)/5.03:_NMR_Spectroscopy.

17. Patiny, Luc. “NMR Predict.” *Nmrdb.org*, www.nmrdb.org/new_predictor/index.shtml?v=v2.87.7.

18. Banfi, Damiano, and Luc Patiny. “Www.nmrdb.org: Resurrecting and Processing NMR Spectra On-Line.” *CHIMIA International Journal for Chemistry*, vol. 62, no. 4, 2008, pp. 280–281., doi:10.2533/chimia.2008.280.

19. Reusch, William. “Visible and Ultraviolet Spectroscopy.” *UV-Visible Spectroscopy*, Michigan State University, 5 May 2013, www2.chemistry.msu.edu/faculty/reusch/VirtTxtJml/Spectrpy/UV-Vis/spectrum.htm.

20. “Ch. 18: Porphyrins.” *Journal of Chromatography Library*, by Erich Heftmann, 5th ed., Elsevier, 1992, p. 337.

21. “High Performance Liquid Chromatography (HPLC).” *Specialty Gases & Specialty Equipment*, Linde, 2020, hiq.linde-gas.com/en/analytical_methods/liquid_chromatography/high_performance_liquid_chromatography.html.

22. Mezencev, Roman. “Re: Until what percentage does DMSO remain not toxic to cells?” *Research Gate*, 2 Feb. 2015,

https://www.researchgate.net/post/Until_what_percentage_does_DMSO_remain_not_toxic_to_cells

23. Stockert, Juan C., et al. “Tetrazolium Salts and Formazan Products in Cell Biology: Viability Assessment, Fluorescence Imaging, and Labeling Perspectives.” Acta Histochemica, Urban & Fischer, 26 Feb. 2018, www.sciencedirect.com/science/article/abs/pii/S0065128117304749.

24. Berridge, Michael V., et al. “Tetrazolium Dyes as Tools in Cell Biology: New Insights into Their Cellular Reduction.” Biotechnology Annual Review, Elsevier, 7 Oct. 2005, www.sciencedirect.com/science/article/pii/S1387265605110047.

25. Mosmann, Tim. “Rapid Colorimetric Assay for Cellular Growth and Survival: Application to Proliferation and Cytotoxicity Assays.” Journal of Immunological Methods, Elsevier, 12 Nov. 2002, www.sciencedirect.com/science/article/abs/pii/0022175983903034.

26. “Photofrin (Porfimer Sodium): Uses, Dosage, Side Effects, Interactions, Warning.” *RxList*, Pinnacle Biologics, Inc., 21 Jan. 2020, www.rxlist.com/photofrin-drug.htm.

27. Reynolds, Tom. “Photodynamic Therapy Expands Its Horizons.” *JNCI: Journal of the National Cancer Institute*, vol. 89, no. 2, 1997, pp. 112–114., doi:10.1093/jnci/89.2.112.

28. Baskaran, Rengarajan, et al. “Clinical Development of Photodynamic Agents and Therapeutic Applications.” *Biomaterials Research*, vol. 22, no. 1, 26 Sept. 2018, doi:10.1186/s40824-018-0140-z.

29. “Foscan.” *European Medicines Agency*, European Public Access Report, 25 Sept. 2018, www.ema.europa.eu/en/medicines/human/EPAR/foscan.

30. Huang, Xiongyi, and John T. Groves. “Oxygen Activation and Radical Transformations in Heme Proteins and Metalloporphyrins.” *Chemical Reviews*, vol. 118, no. 5, 2017, pp. 2491–2553., doi:10.1021/acs.chemrev.7b00373.

31. Li, Zongxi, et al. “Non-Invasive Transdermal Two-Dimensional Mapping of Cutaneous Oxygenation with a Rapid-Drying Liquid Bandage.” *Biomedical Optics Express*, vol. 5, no. 11, 2014, pp. 3748–3764., doi:10.1364/boe.5.003748.

32. “1.2 The Solar Resource.” *Electricity from Sunlight: An Introduction to Photovoltaics*, by Paul A. Lynn, Wiley, 2010, p. 6.

33. “2.4 Other Cells and Materials.” *Electricity from Sunlight: An Introduction to Photovoltaics*, by Paul A. Lynn, Wiley, 2010, p. 71.

34. “How a Solar Cell Works.” *ChemMatters*, American Chemical Society, www.acs.org/content/acs/en/education/resources/highschool/chemmatters/past-issues/archive-2013-2014/how-a-solar-cell-works.html.

35. “Chapter Two: Dye-Sensitized Solar Cell Fundamentals.” *Towards Efficient Photovoltaic Devices: Key Facts and Experiments on Dye-Sensitized Solar Cells*, by Codrin Alexandru Andrei, Cambridge Scholars Publishing, 2017, p. 29.

36. “Reference Air Mass 1.5 Spectra.” *NREL.gov*, U.S. Department of Energy, www.nrel.gov/grid/solar-resource/spectra-am1.5.html.

37. Namba, Susumu, and Yasushi Hishiki. “Color Sensitization of Zinc Oxide with Cyanine Dyes.” *The Journal of Physical Chemistry*, vol. 69, no. 3, 1965, pp. 774–779., doi:10.1021/j100887a010.

38. Li, Xing-Yu, et al. “A Comparative Study of Porphyrin Dye Sensitizers YD2-o-C8, SM315 and SM371 for Solar Cells: the Electronic Structures and Excitation-Related Properties.” *The European Physical Journal D*, vol. 70, no. 10, 18 Oct. 2016, doi:10.1140/epjd/e2016-70071-3.

39. Lu, Jianfeng, et al. “Push-Pull Zinc Porphyrins as Light-Harvesters for Efficient Dye-Sensitized Solar Cells.” *Frontiers in Chemistry*, vol. 6, 16 Nov. 2018, doi:10.3389/fchem.2018.00541.

40. Song, Heli, et al. “Porphyrin-Sensitized Solar Cells: Systematic Molecular Optimization, Coadsorption, and Cosensitization.” *Chemical Communications*, vol. 54, no. 15, 2018, pp. 1811–1824., doi:10.1039/c7cc09671b.